# Continental-scale geochemical survey of lead (Pb) in mainland China's pedosphere: Concentration, spatial distribution and influences

Xueqiu Wang[a,b], Zhixuan Han[a,b,*], Wei Wang[a,b], Bimin Zhang[a,b], Hui Wu[a,b], Lanshi Nie[a,b], Jian Zhou[a,b], Qinghua Chi[a,b], Shanfa Xu[a,b], Hanliang Liu[a,b], Dongsheng Liu[a,b], Qingqing Liu[a,b]

[a] Key Laboratory of Geochemical Exploration, Institute of Geophysical and Geochemical Exploration, CAGS, Langfang, Hebei, 065000, China
[b] UNESCO International Center on Global-scale Geochemistry (ICGG), Langfang, Hebei, 065000, China

ABSTRACT

The China Geochemical Baseline (CGB) project (2008–2012) obtained comparable, continental-scale, geochemical data including lead (Pb) concentrations in the pedosphere. Some 3382 topsoil samples were collected at depths of 0–25 cm. Lead concentrations in soil were determined by inductively coupled plasma mass spectrometry (ICP-MS) using 4-acid extraction under strict quality control. The median Pb concentration throughout China was 22.1 mg/kg and varied between 15.6 and 30 mg/kg according to the morphological landscape. There were predominantly low Pb concentrations in northwestern China and much higher concentrations in southeastern China. This is mainly due to differences in climate and landscape, geology (parent rocks) and the presence of mineralization. The arid and semi-arid landforms in northern and northwestern China had low Pb concentrations. High Pb concentrations were most often linked to geology (occurrence of granite) and climate. The most important Pb anomalies occurred in the southern and southwestern parts of China in areas with known polymetallic mineralization. Such anomalies may be further enhanced by mining or smelting activities.

## 1. Introduction

Lead (Pb) is a potentially toxic element that is part of a suite of elements often incorrectly called 'heavy metals' (Duffus, 2002; Chapman, 2007) and has received particular attention in recent decades (Reimann et al., 2012a; Zhu et al., 2013a, b; Bi et al., 2015a, b; Marx et al., 2016; Fabian et al., 2017; Kushwaha et al., 2018). Exposure to Pb can cause serious toxic reactions (Chiodo et al., 2007). According to Needleman (2004), 0.6% of the world's disease burden is caused by Pb pollution, and the World Health Organization (WHO, 2016) reported that, in 2013, there were 853,000 Pb-related deaths worldwide. The situation is more serious in developing countries than developed ones (WHO, 2016). As the largest developing country, and one that generates large Pb emissions, China should pay more attention to the increased Pb levels in blood (Han et al., 2018), which are of particular concern for children (Li et al., 2012). Many studies have demonstrated that there is a significant correlation between Pb concentrations in blood and those in soil or sediments (Ren et al., 2006; Mielke et al., 2007; Laidlaw and Taylor, 2011). To manage and prevent Pb poisoning, it is vital to know the concentration and spatial distribution of Pb in the pedosphere (Mielke et al., 2011). However, very little research has addressed Pb pollution in China at the national level.

The pedosphere is the outermost layer of the Earth that is composed of soil and subject to soil formation processes. Humans have investigated the concentration and spatial distribution of elements in the pedosphere for the past 100 years. To date, average concentrations of Pb in the upper crust have been extensively studied (Clarke, 1889; Clarke and Washington, 1924; Goldschmidt, 1954; Taylor, 1964; Shaw et al., 1986; Wedepohl, 1995; Rudnick and Gao, 2003). However, little is known of its spatial distribution in the Earth's surface or near-surface environments (Wang et al., 2016). Therefore, Darnley et al. (1995) proposed the Global Geochemical Baselines project to obtain comparable continental-scale geochemical data across national borders (Reimann et al., 2012b). China developed the leadership and funding to take this project forward (Xie and Cheng, 2001; Smith et al., 2012; Yao et al., 2014). The China Geochemical Baseline (CGB) project was initiated from 2008 to 2012 and covers all of China (Wang, 2012; Wang et al., 2015a). In the CGB project, catchment sediments or alluvial soils were selected as the best sampling media for representing the distribution of elements in continental-scale geochemical surveys (Xie and

Cheng, 1997; Salminen, 2005; Caritat et al., 2009, 2018; Wang et al., 2015a).

Landscape, geological background (parent rocks), quaternary materials, vegetation cover, climate (especially precipitation) and, last but not least, human activities, such as land use, population and traffic density, and the distribution of major industries, all need to be considered when interpreting geochemical maps at the continental scale (Reimann et al., 2012b). To provide all this information is beyond the scope of this paper. This study uses data from the CGB project to 1) present the concentration and spatial distribution of Pb in the Chinese pedosphere, and 2) investigate influences such as geological background, landscape, climate, and mineralization.

## 2. Materials and methods

### 2.1. Sample collection

Selecting the optimal sampling media is a critical problem in establishing geochemical baselines over very large areas, in this case, 9.6 million km$^2$. In the CGB project, catchment sediments and alluvial soils were selected because they can provide high-resolution and comparable baseline data nationwide (Xie and Cheng, 1997; Salminen, 2005; Caritat et al., 2009, 2018; Wang et al., 2015a). The sampling methodology was developed for China's diverse terrain, which includes mountains, hills, plains, deserts, grassland, loess and karst terrain. Specifically, the sampling media were: 1) floodplain sediment or alluvial soil from plains and hilly terrain near exorheic rivers in eastern China, 2) overbank sediment from exorheic river systems in mountainous terrain in southwestern China, and 3) catchment basin and lake sediments from desert and semi-desert terrains, respectively. Sampling was conducted from 2008 to 2012. Two sampling sites were allocated to each CGB grid cell of 1° (longitude) × 40′ (latitude), approximately equal to 80 × 80 km$^2$ in size. Top samples are generally collected from the A-horizon at depths of 0–25 cm. Each sample is composited from three samples collected at the vertex of an equilateral triangle with 50 m on a side. The weight of each sample was about 5 kg. The number of field duplicate samples exceeded 3% of the total number of samples. In total, 3382 samples were collected from 1500 CGB grid cells at an average density of 1 per 3000 km$^2$ across mainland China (See Fig. 1).

Details of the sampling media, site distribution, and quality control are provided in our previous work (Wang et al., 2015a).

### 2.2. Laboratory analysis and data quality control

All samples were air-dried and sieved through a 2 mm nylon mesh screen in the laboratory. Samples were subsequently ground to < 74 μm (200 mesh) in an agate mill for analysis. Sample analysis was conducted in the IGGE laboratory (Institute of Geophysical and Geochemical Exploration).

A 0.250 g aliquot was weighed and placed into a 25 ml test tube to which 10 ml HF, 5 ml HNO$_3$, 2 ml HClO$_4$ and 8 ml of aqua regia were added. The test tube was heated in a boiling water bath for 1 h and shaken once during the course of decomposition. After cooling, 1 ml supernatant was diluted with HNO$_3$ solution (2%) to 10 ml. Then, the solution was used to determine the total Pb concentration by inductively coupled plasma mass spectrometry (ICP-MS). The detection limit was 2 mg/kg and the reportable rate was as high as 100%.

The standardized quality control (QC) procedures consisted of 1) field training for all sampling participants; 2) field sampling checking by random selection of more than 5% of the sampling sites; 3) collection of 3% field duplicate samples; 4) blank insertion of 10% laboratory replicate samples; and 5) insertion of four standard reference materials into each batch of 50 routine samples (Caritat et al., 2018). The passing percentage rates of national standard reference materials, laboratory replicate samples and field duplicates were 100%, 99.9%, and 99.5%, respectively. The Pb analytical scheme and quality monitoring system for the CGB project are described in detail elsewhere ( Zhang et al., 2012; Wang et al., 2015a). In summary, the CGB project obtained high-quality Pb data.

### 2.3. Data analysis and mapping

Geochemical maps of Pb were drawn up using Geoexpl2012 software, which was developed by the Development and Research Center of the China Geological Survey. Raw analytical data were interpolated to generate a regular output grid of 80 × 80 km using an exponentially-weighted moving average model (Wang et al., 2015). Eighteen-shade color map classes were created according to the following percentile Pb
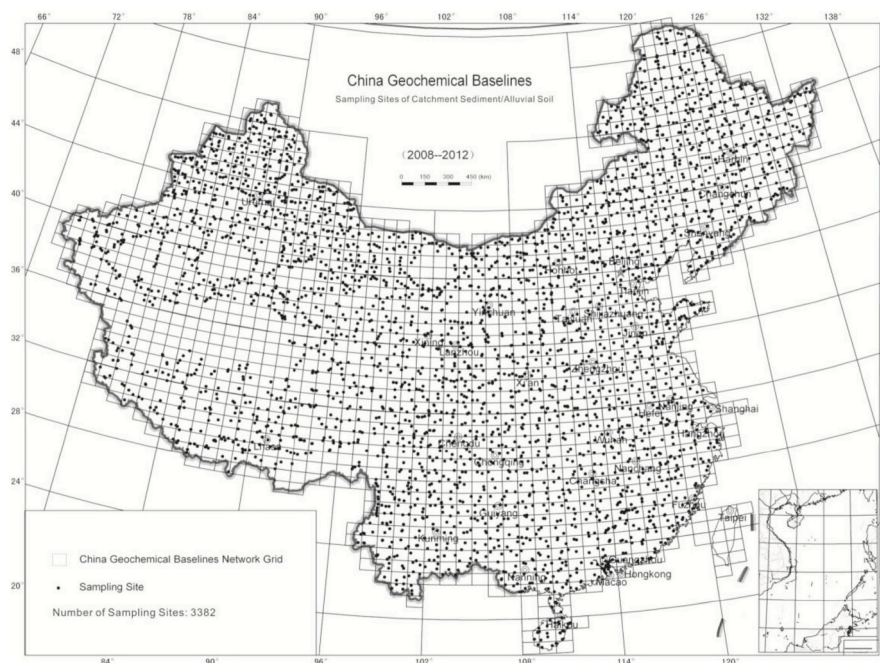


**Fig. 1.** Map of CGB project sampling sites.

**Table 1**
Percentiles of Pb concentrations (mg/kg) found in top sediment/alluvial soil samples from the CGB project.

| N | Min | P2.5 | P25 | P50 | P75 | P85 | P97.5 | Max | AM | GM | STD |
|---|-----|------|-----|-----|-----|-----|-------|-----|-----|-----|-----|
| 3382 | < 2.0 | 11.8 | 17.6 | 22.1 | 28.2 | 34.4 | 72.1 | 1386 | 29.3 | 23.6 | 48.7 |

Notation: N = number of samples; P = percentile (P50 = median); Min = minimum; Max = maximum; AM = arithmetical mean; GM = geometric mean; STD = standard deviation.
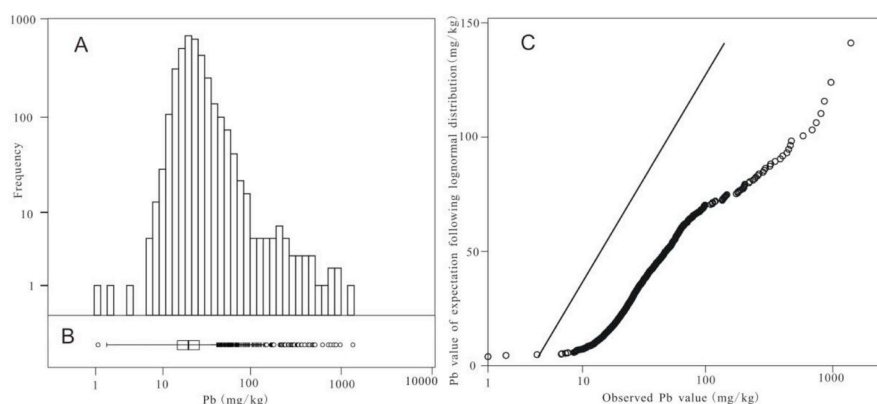


**Fig. 2.** Histograms (A), boxplot(B), and Q-Q plot (C) displaying the distribution of Pb concentrations (mg/kg) in top sediment/alluvial soil samples of the CGB project.

concentrations: P2.5, P5, P10, P15, P20, P25, P30, P40, P50, P60, P70, P75, P80, P85, P90, P95, and P97.5, which are equivalent to 11.8, 13.0, 14.6, 15.6, 16.7, 17.6, 18.5, 20.2, 22.1, 24.1, 26.6, 28.2, 30.9, 34.4, 40.6, 54.6, and 72.1 mg/kg.

The data was statistically analyzed using the statistical package SPSS v17.0 (SPSS Inc.). Correlation analysis between Pb and $Al_2O_3$, CaO, MgO, $Na_2O$, $K_2O$, $Fe_2O_3$, MnO concentration was carried out without the outliers of Pb concentration (lower than P2.5 and higher than P97.5). The database of the major elements ($Al_2O_3$, CaO, MgO, $Na_2O$, $K_2O$, $Fe_2O_3$, and MnO) is available at http://www.globalgeochemistry.com/en/index.php.

## 3. Results

### 3.1. General abundance of Pb in China

Summary statistics of Pb concentrations determined by the CGB project are shown in Table 1. Pb concentrations ranged from < 2 to 1386 mg/kg, with a median of 22.1 mg/kg. The average concentration was 29.3 mg/kg (95% confidence interval, CI: [27.7, 30.9] mg/kg). The 95% range (P2.5–P97.5) of Pb concentrations was 11.8–72.1 mg/kg. The median Pb concentration is comparable to that found by the Environmental Geochemical Monitoring Networks (EGMON) project (23 mg/kg, Xie and Cheng, 2001), which was a continental-scale geochemical baseline study conducted in 1994–1996 (Cheng et al., 1997).

The histograms show approximately lognormal distributions (Fig. 2), which suggests that Pb concentrations may be mainly related to natural factors and only slightly influenced by human activities. The

geometric mean value of Pb in this study was 23.6 mg/kg, which is just a little lower than the background value reported for Chinese topsoil (26 mg/kg; CNEMC, 1990) and that reported for Chinese stream sediments (27 mg/kg; Chi and Yan, 2007). There were 15.21% samples with Pb concentrations higher than the Grade I Chinese Soil Guideline (35 mg/kg), while 2.16% exceeded the Grade II Chinese Soil Guideline for agricultural soils (80 mg/kg).

The Pb concentrations reported in various loose sediments in China are summarized in Table 2. They are ranked as follows: agricultural soil (25.6 mg/kg, data from the First National Soil Pollution Survey, Chen et al., 2015) > topsoil (23.5 mg/kg, CNEMC, 1990) > > urban soils of 31 metropolises (23.4 mg/kg, Cheng et al., 2014) > floodplain sediments (23mg/kg, data from EGMON project, Xie and Cheng, 2001).

Pb concentrations in the continental crust and rocks are summarized in Table 3. The Pb concentration in the Chinese pedosphere (29.3 mg/kg, this study) is higher than those in the continental crust, which vary from 8 to 16 mg/kg. This indicates that Pb could be enriched in the soil formation process. In terms of rock types, Pb concentrations in granite are the highest, followed by shale, schist, sandstone, slate, phyllite, gneiss, intermediate rocks, siliceous rocks, basic rocks, carbonate rocks, marble, and ultramafic rocks (Table 3). It could be concluded that the more acidic the rock is, the higher the Pb concentration.

### 3.2. General spatial distribution of Pb and its influences in China

The most noticeable pattern in the Pb distribution shown on the geochemical map of topsoil samples (Fig. 3) is an increasing trend of Pb concentration from the northwest to southeast. Latitude 32° N can be

**Table 2**
Pb concentration (mg/kg) in various loose sediments throughout China.

| Soil type | Sample size | Parameter | Pb concentration | Reference |
|-----------|-------------|-----------|------------------|-----------|
| Topsoil | 4095 | M | 23.5 | CNEMC (1990) |
| Floodplain sediments | 529 | M | 23 | Xie and Cheng (2001) |
| Agricultural Soil | 38393 | M | 25.6 | Chen et al. (2015) |
| Stream sediments | 869 | AM | 27 | Chi and Yan (2007) |
| Urban soil of 31 metropolises | 1011 | M | 23.4 | Cheng et al. (2014) |

Notation: AM = arithmetical mean; M = median.

**Table 3**
Pb concentration (mg/kg) in continental crust and rocks.

| Type | | Pb | Reference |
|---|---|---|---|
| Crust | Continental crust | 16 | Goldschmidt, 1933 |
| | Continental crust | 16 | Vinogradov (1962) |
| | Continental crust in eastern China | 15 | Chi and Yan (2007) |
| | Continental crust | 14.8 | Wedepohl (1995) |
| | Continental crust | 12.5 | Taylor (1964) |
| | Continental crust | 11 | Rudnick and Gao (2003) |
| | Continental crust | 8 | Taylor and McLenan, 1985 |
| Rocks | Granites in China | 26 | Yan and Chi (2005) |
| | Granites in China | 26 | Shi et al. (2005) |
| | Acidic rocks in China | 24 | Yan and Chi (2005) |
| | Shales in eastern China | 23 | Yan and Chi (2005) |
| | Acidic rocks | 20 | Vinogradov (1962) |
| | Schists in eastern China | 19 | Chi and Yan (2007) |
| | Sandstones in eastern China | 18 | Yan and Chi (2005) |
| | Slates in eastern China | 18 | Chi and Yan (2007) |
| | Phyllites in eastern China | 18 | Chi and Yan (2007) |
| | Gneisses in eastern China | 16 | Chi and Yan (2007) |
| | Intermediate rocks in China | 15.5 | Chi and Yan (2007) |
| | Siliceous rocks in eastern China | 14 | Chi and Yan (2007) |
| | Basic rocks in China | 13 | Yan and Chi (2005) |
| | Carbonate rocks in eastern China | 8.7 | Yan and Chi (2005) |
| | Marbles in eastern China | 8.6 | Chi and Yan (2007) |
| | Ultramafic rocks in China | 8 | Yan and Chi (2005) |

used to divide mainland China into southern and northern China. The median values of Pb are 30.97 and 19.73 mg/kg in the south and north, respectively, with the Pb-south:Pb-north ratio being 1.57.

Low Pb concentrations (here defined as Pb content < P25; blue regions on map, Fig. 3) are distributed in arid and semi-arid areas (arid desert basins, Gobi Desert, semi-desert grassland and loess) in the northern and northwestern parts of China. Here, the soil is mostly composed of windblown sand and is unpolluted or only slightly polluted by human activities (Wei et al., 1991; Zhou et al., 2015; Wang et al., 2015a).

High Pb concentrations (Pb content > P75; yellow regions on map) can be interpreted as a lithological effect. It will be discussed later in this paper.

Pb anomalies (Pb content > P85; orange and red regions of the map), both in upper and deeper samples, were mainly distributed in the southern and southwestern parts of China. These anomalies were caused by a combination of geological background, climate, and landscape. They are especially associated with mineralization, such as that of the Gangdise metallogenic belt, the Nujiang-Lancangjiang-Jinshajiang metallogenic belt, the metallogenic province at the southwestern border of the Yangtze Plate, and the southeastern coastal metallogenic belt, which all have many lead-zinc deposits (Hu et al., 2007; Huang et al., 2011; Mao et al., 2002; Zhang et al., 2013).

Pb anomalous centers (Pb content > P97.5; dark red regions of the map) were exactly correlated with polymetallic mineralization or polymetallic mining activities. These occur in areas such as A-H in Fig. 3. Pb concentration in topsoil sample was as high as 809 mg/kg near the Baiyinnuoer Pb−Zn deposit (A in Fig. 3), which is more than 40 times the background concentration of Pb in Inner Mongolia (CNEMC, 1990). This higher concentration is probably due to mining activities. However, it cannot be ignored that some deposits, which mainly located in North China, are only marked by weak anomalies. This is mainly due to the lower geochemical background of Pb in North China.

## 4. Discussion

### 4.1. Comparison of Pb concentrations in different countries

Pb concentrations vary greatly in different countries and regions. China and Australia, and American and European countries, have all conducted continental-scale geochemical surveys (Caritat et al., 2018), including the EGMON (Cheng et al., 1997) and CGB projects in China (Wang et al., 2015a), the National Geochemical Survey of Australia (NGSA) (Caritat and Cooper, 2011; Reimann and Caritat, 2017), the Soil Geochemical Landscapes (SGL) project in the conterminous United States (Smith et al., 2013), and the Forum of European Geological Surveys (FOREGS) (Salminen, 2005) and Geochemical Mapping of Agricultural Soils (GEMAS) projects in Europe (Reimann et al., 2012a, 2014a,b). Table 4 summarizes comparable data for Pb in loose sediments or soils from these projects (Liu et al., 2015; Caritat et al., 2018). Chi and Yan (2007) reported that the arithmetic mean Pb concentration
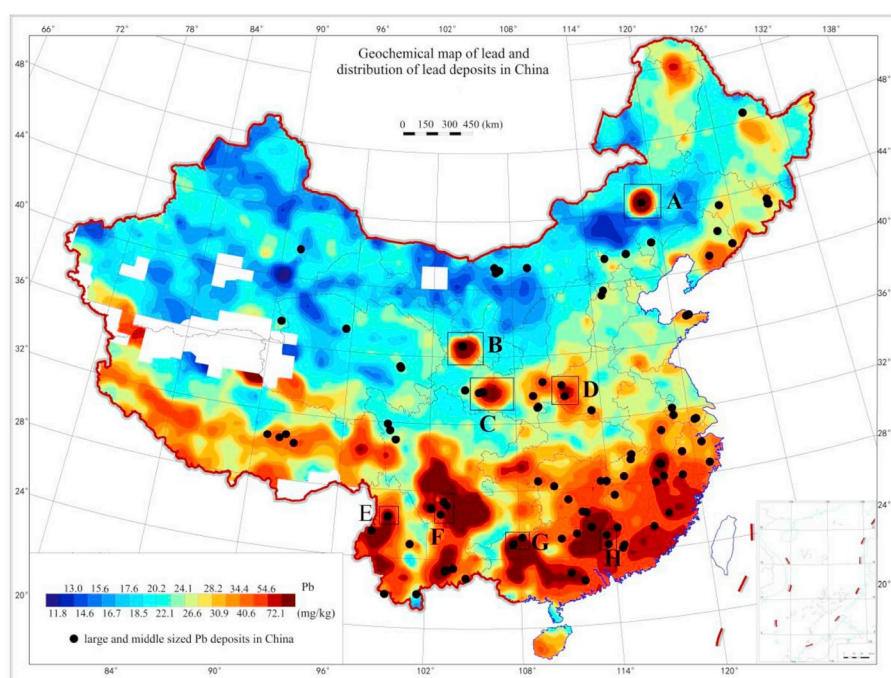


**Fig. 3.** Distribution of moderate and large Pb deposits in geochemical map of top sediment/alluvial soil samples in China. Baiyinnuoer Pb−Zn deposit in Inner Mongolia (A), Lanzhou-Baiyin Ag−Pb−Zn ore-field in Gansu (B), Fengxian Pb−Zn ore-field in Shannxi (C), Lingbao-Lushi Pb−Zn ore-field in Henan (D), Huize Pb−Zn ore-field (F) and the largest Pb−Zn deposit in Asia- Jinding Pb−Zn ore-field(E) in Yunnan, Hechi Pb−Zn ore-field in Guangxi (G), Fankou Pb−Zn ore-field in Guangdong (H).

**Table 4**

Total Pb concentrations (mg/kg) in loose sediments of China, Australia, USA, and Europe.

| Region (Survey) | Sample type | N | Analytical method | Parameter | Pb (mg/kg) | References |
|---|---|---|---|---|---|---|
| China | Catchment sediments and alluvial soil | 3382 | ICP-MS (HF + $HNO_3$ + $HClO_4$ + aqua regia) | M | 22.1 | This study |
| | Floodplain sediments | 529 | ICP-MS (HF + $HNO_3$ + $HClO_4$ + aqua regia) | M<br>Range | 23<br>2.9–201.4 | Xie and Cheng , 2001 |
| USA | Soil | 4841 | ICP-MS (HF + HCl + $HNO_3$ + $HClO_4$) | AM<br>M<br>Range | 25.8<br>18.1<br>< 0.5–12400 | Smith et al. (2013) |
| Australia | Top catchment outlet sediments | 1315 | ICP-MS (HF + $HNO_3$) | M<br>range | 12.9<br>0.5–1530 | Caritat and Cooper (2011) |
| Europe (GEMAS) | Agricultural soil | 2211 | XRF (Fusion) | M<br>range | 21<br>< 3–1309 | Reimann et al. (2012b) |
| Europe (FOREGS) | Topsoil | 843 | XRF (Fusion) | M<br>AM<br>Range | 22.6<br>32.6<br>5.3–970 | Salminen (2005) |
| | Floodplain sediments | 747 | | M<br>AM<br>Range | 22<br>54.1<br>4.0–7080 | |

Notation: N = number of the samples; AM = arithmetic mean; GM = geometric mean; M = median.

in stream sediments in China was 27 mg/kg, which is lower than that in Europe (38.6 mg/kg, Salminen, 2005). The median concentration of Pb in China (23 mg/kg in the EGMON project and 22.1 mg/kg in the CGB project) is similar with that in Europe (22 mg/kg in the FOREGS project) (Table 4). In Europe, the FORGES project reported floodplain sediments to have similar topsoil Pb concentrations to those in agricultural soils (as reported by the GEMAS project; Salminen, 2005; Reimann et al., 2012a). The median concentrations of Pb in loose sediments or soils in the USA (18.1 mg/kg) and Australia (12.9 mg/kg) are relatively low (see Table 4).

### 4.2. Factors influencing Pb concentration and distribution in China

#### 4.2.1. Geomorphologic landscapes

The geomorphologic landscape plays an important role in the supergene geochemical behavior of Pb (Fortescue, 1992; Yin, 1999). The landscape varies significantly across China, as shown in Fig. 4. Hilly or low mountainous areas, alluvial plains, and forests are distributed in eastern and northeastern China. Arid desert terrain, including desert basins, the Gobi Desert, semi-desert grassland and loess plateaus, are concentrated in northern and northwestern China. Southwestern China
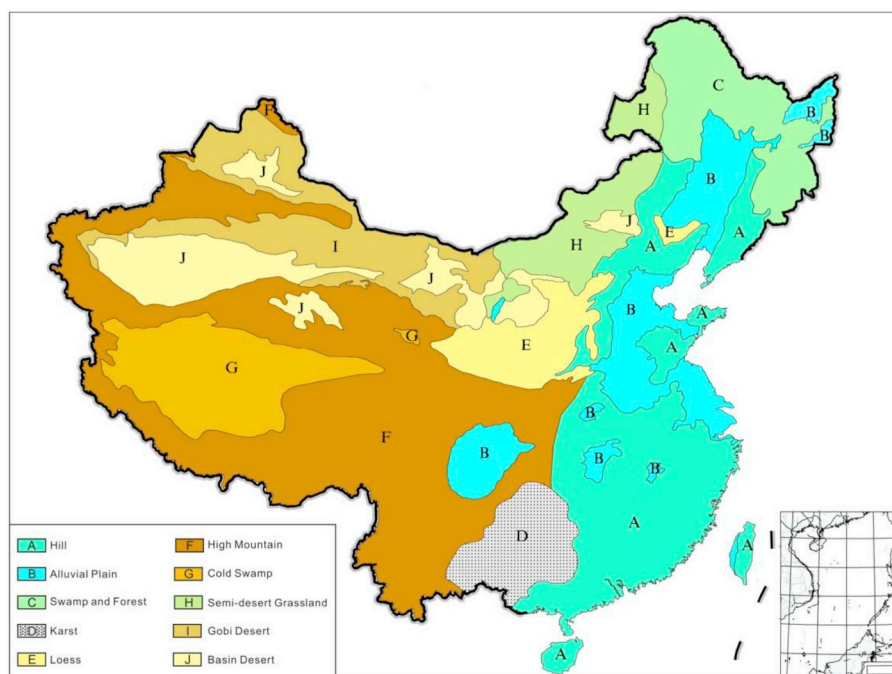


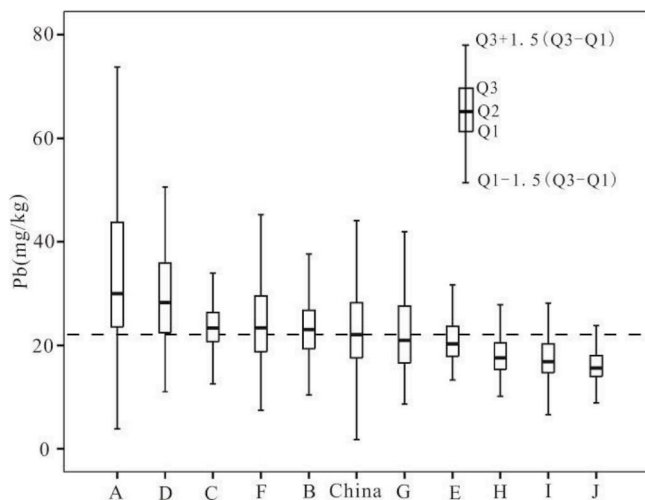**Fig. 4.** Geomorphologic landscape terrains in China (after Wang et al., 2015b).

**Fig. 5.** Boxplots displaying statistical variation of Pb concentration (mg/kg) in top sediment/alluvial soil samples in different geomorphological terrains of China.

is dominated by high mountains. The Pb statistics for different landscapes are listed in Fig. 5 and Table 5. The median Pb concentrations of ten surveyed landscapes are very broad, ranging from 15.6 to 30.0 mg/kg, which indicates the influence of the geomorphological landscape on Pb distribution. Karst and hilly terrain have the highest median Pb concentrations among these landscapes in both upper and deeper samples, while desert basins have the lowest. The high Pb values in the karst terrain are due to Pb becoming enriched in red earth and laterite during the process of the chemical decomposition of carbonates (Yin, 1999), and Pb−Zn mineralization in southwestern China where karst terrain occurs. The low Pb values in desert basin terrain are due to the dominance of quartz-rich windblown sand in the samples (Reimann et al., 2012a).

#### 4.2.2. Parent materials or geological background

Elemental distribution patterns in continental-scale geochemical maps are mainly determined by natural variation (Reimann et al., 2009). Parent material controls at least 50% of the variability in soil Pb (Yin, 1999; Reimann et al., 2012a; Fabian et al., 2017). Pb is mainly hosted as an isomorphism in the lattice of potash feldspar and biotite, which are rock-forming minerals. In the soil formation process, some potash feldspar and biotite are preserved and some are converted to clay minerals like illite. These minerals have one thing in common—they all contain Al and K. Correlation analysis shows that Pb concentrations were significantly correlated to $Al_2O_3$ and $K_2O$

**Table 6**
Results of correlation analysis ($R^2$) between Pb and $Al_2O_3$, $K_2O$, $Fe_2O_3$, MnO concentrations.

| | $Al_2O_3$ | $K_2O$ | $Fe_2O_3$ | MnO |
|---|---|---|---|---|
| Pb | 0.432[**] | 0.263[**] | 0.306[**] | 0.170[**] |

[**]$p < 0.01$.

(Table 6), indicating that Pb concentration is determined by the parent materials. The significant positive correlation between the concentration of Pb and $Fe_2O_3$ and MnO may be because Pb can be adsorbed on the surface of Fe−Mn oxides (Han et al., 2012).

Granites are more enriched in Pb than other rock types (see Table 3). To further study the influence of geological background on Pb concentration, the spatial distribution of the correlation between Pb concentration and granites is shown in Fig. 6. High Pb concentrations match well with the granite distribution outline, especially in the Mesozoic giant granites province in South China, on the concentration map of Pb (see Fig. 6).

#### 4.2.3. Climate or weathering

The CIA is widely used as an indicator of the degree of weathering of source areas (e.g. Kasanzu et al., 2008; Négrel et al., 2015). The weathering history of CGB topsoil samples was evaluated using the chemical index of alteration (CIA), defined by Nesbitt and Young (1982) as $CIA = [mAl_2O_3/(mAl_2O_3 + mCaO^* + mNa_2O + mK_2O)] \times 100$. Where m represents molar proportions, and $CaO^*$ silicate-borne CaO. Due to lack of data, this fraction of silicate-borne CaO could not be calculated for both datasets discussed here. Therefore, we observe a certain bias due to Ca bound in carbonates and gypsum at continental-scale. Areas underlain by, or containing, carbonates and gypsum have very low CIA values (Reimann et al., 2012b). The calculated CIA values show that most of the CGB topsoil samples fall within the intermediate and low weathering range (45% of the samples had CIA values of 60–80, 27% had 40–60), and 20% of soils had low CIA values ($< 50$), while less than 8% of the samples were in the intense weathering range (80–100) (Servaraj and Arthur, 2006). Chemical weathering processes play an important role in elemental transportation and soil formation. Because Ca, Na, and Mg are removed from the soil profile during soil development (Négrel et al., 2015), Pb concentration (varying from P2.5 to P97.5) has a significantly negative correlation with $Na_2O$, CaO, and MgO concentration (Table 7). According to the scatter plot in Fig. 7, Pb concentration (varying from P2.5 to P97.5) is found to have an exponential relationship with CIA. Weathering (soil formation) leads to an increase in Pb concentration in soils. The results suggest that the Pb distribution is related to climate or weathering.

**Table 5**
Characteristics of Pb concentration (mg/kg) in top sediment/alluvial soil samples in the different landscapes of China.

| Landscape | N | Min | P25 | P50 | P75 | P85 | Max | AM | GM | STD |
|---|---|---|---|---|---|---|---|---|---|---|
| Whole China | 3382 | 1 | 17.6 | 22.1 | 28.2 | 34.4 | 1385.6 | 29.3 | 23.6 | 48.7 |
| Hill (A) | 633 | 3.8 | 23.6 | 30 | 43.7 | 54.4 | 808.7 | 39.6 | 32.7 | 46.2 |
| Karst (D) | 126 | 11.1 | 22.5 | 28.3 | 35.8 | 41.9 | 1385.6 | 53.6 | 23.1 | 7.8 |
| Swamp and forest (C) | 218 | 10.7 | 20.8 | 23.4 | 26.3 | 28.3 | 147.5 | 24.6 | 23.6 | 10.2 |
| High mountain (F) | 923 | 1 | 18.8 | 23.4 | 29.6 | 36.1 | 859.5 | 33.4 | 32.2 | 141 |
| Alluvial plain (B) | 335 | 10.4 | 19.4 | 23.1 | 26.8 | 29.4 | 70.3 | 24.1 | 21.5 | 72.8 |
| Cold swamp (G) | 140 | 8.6 | 16.6 | 21 | 27.6 | 32 | 290 | 25.9 | 25.4 | 55.7 |
| Loess (E) | 170 | 13.3 | 17.9 | 20.3 | 23.6 | 26.3 | 968 | 27.2 | 22.3 | 25.5 |
| Semi-desert grassland (H) | 215 | 10.1 | 15.4 | 17.6 | 20.5 | 22.3 | 39.6 | 18.3 | 17.8 | 4.4 |
| Gobi Desert (I) | 424 | 6.6 | 14.8 | 16.9 | 20.3 | 22.1 | 35.8 | 17.6 | 17.1 | 4.4 |
| Basin desert (J) | 198 | 1.8 | 14 | 15.6 | 18 | 19.9 | 26.2 | 16.1 | 15.6 | 3.8 |

Notation: N = number of samples; P = percentile (P50 = median); Min = minimum; Max = maximum; AM = arithmetic mean; GM = geometric mean; STD = standard deviation.
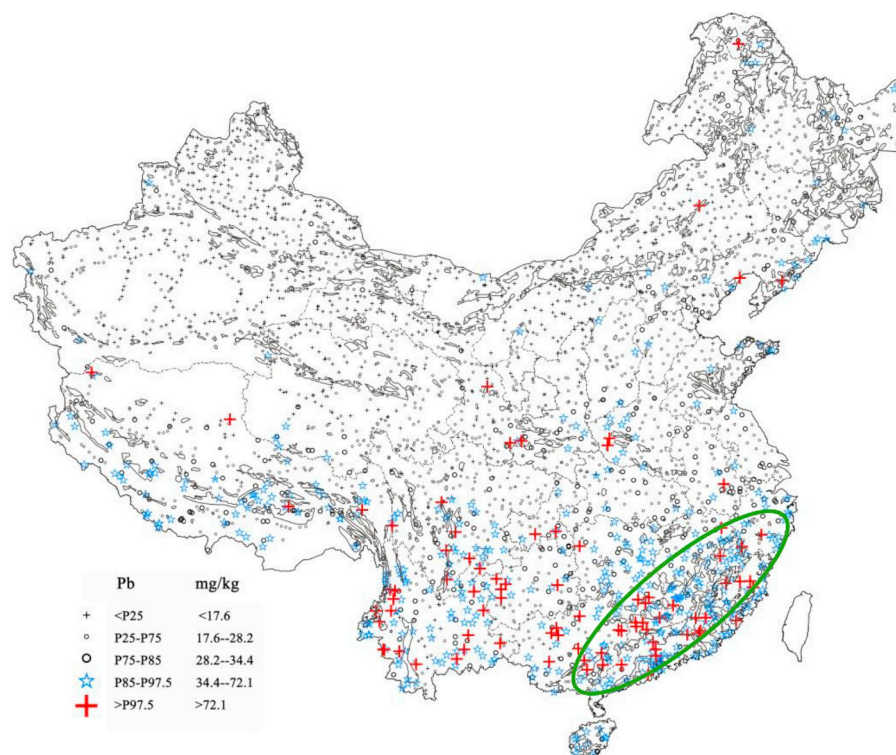
**Fig. 6.** Map of Pb concentration in top sediment/alluvial soil samples of the CGB project, and granite distribution in China (Green ellipse-Mesozoic giant granite province in South China). (For interpretation of the references to color in this figure legend, the reader is referred to the Web version of this article.)

**Table 7**
Results of correlation analysis ($R^2$) between Pb and MgO, Na$_2$O, CaO concentrations.

| | MgO | Na$_2$O | CaO |
|---|---|---|---|
| Pb | $-0.183^{**}$ | $-0.304^{**}$ | $-0.305^{**}$ |

$^{**}p < 0.01$.
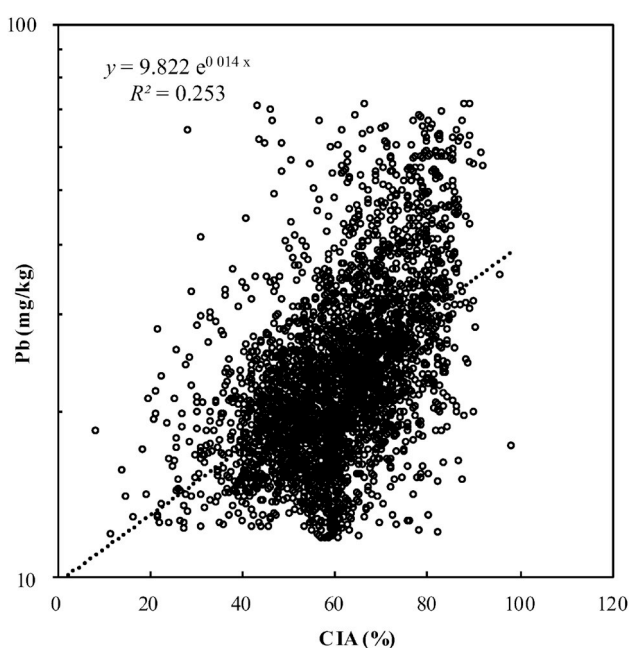


**Fig. 7.** Scatterplot of Pb concentration vs. CIA.

#### 4.2.4. Pb mineralization

Ore-forming processes commonly affect large areas of the earth's crust, resulting in large-scale geochemical anomalies (Wang et al., 2007). In the European GEMAS project, it was observed that Pb anomalies coincide with known Pb mineral belts or deposits (Reimann et al., 2012a). A similar conclusion was reached in this study: that nearly 80% of the extremely high Pb concentrations (red cross in Fig. 8) fall in the Pb metallogenic belt. This further indicates that most Pb anomalies (dark red color in Fig. 3) are exactly correlated with polymetallic mineralization. Moreover, smelting plants are always located near the deposits, and smelting activities could enhance the pollution level of Pb (Li et al., 2014; Bi et al., 2017).

### 5. Conclusions

This paper provides the first continental-scale geochemical survey of the general abundance and distribution of Pb in the Chinese pedosphere. The 95% range (P2.5–P97.5) of Pb concentrations was 11.8–72.1 mg/kg with a median value of 22.1 mg/kg. The spatial distribution pattern of Pb shows an increasing trend from the northwest to southeast. Low Pb concentrations are distributed in the arid and semi-arid landforms of the northern and northwestern parts of China. Weathering (soil formation) leads to an increase in Pb concentration in soils. Landscapes play an important role in the supergene geochemical behavior of Pb. High Pb concentrations match well with the distribution of granite, and Pb anomalies are mainly distributed in southern and southwestern parts of China. These are mainly related to climate and polymetallic mineralization, which is probably enhanced by mining and smelting activities. A significant correlation between Pb and Al$_2$O$_3$, K$_2$O, Fe$_2$O$_3$, and MnO concentrations indicates that the spatial distribution of Pb is associated with parent rocks. Taken together, these results suggest that the concentration and distribution of Pb are predominantly related to parent materials, landscape, climate, and mineralization.
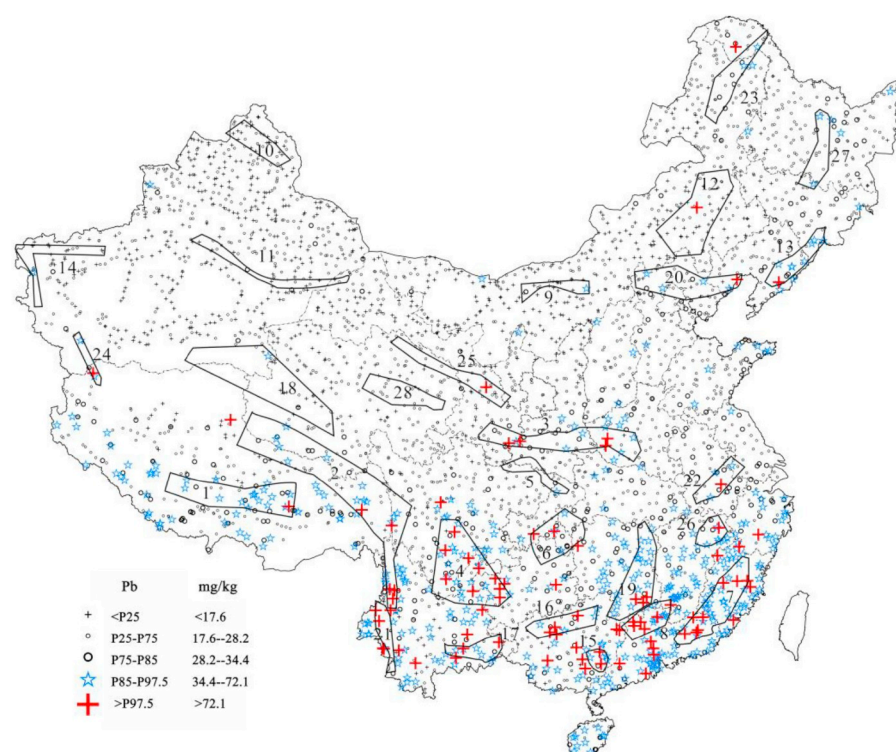
**Fig. 8.** Map of Pb concentrations in the top sediment/alluvial soil samples of the CGB project, and the Pb metallogenic belt (Zhang et al., 2013). 1-Gangdise in Tibet, 2-Sanjiang area in southwestern China, 3-Qilian-Qinling orogenic belt, 4-junction area of Sichuan, Yunnan and Guizhou, 5-North verge of Yangtze platform, 6-western Hunan and Hubei, 7-southern Fujian and eastern Guangdong, 8-southern Jiangxi and northern Guangdong, 9-Langshan mountain and Zhaertai area, 10-Altay, Xinjiang, 11-East Tianshan, Xinjiang, 12-Tuquan-Ongniud Banner in Daxinganling, 13-southern Jilin and northern Liaoning, 14-Kashi-Hetian in Xinjiang, 15-eastern Guangxi and western Guangdong, 16-Hechi-Rongxian in northern Guangxi, 17-Honghe-Wenshan in southeastern Yunnan, 18-eastern Kunlun orogenic belt, 19-eastern Hunan and western Jiangxi, 20-Yanshan-Liaoning area, 21-Changning-Lancang area in Yunnan, 22-middle and lower Yangtze River, 23-Derbugan-Sanhe area in Inner Mongolia, 24-southern Tarim basin, 25-northern Qilian orogenic belt, 26-northern Wuyi mountain, 27-Xiaoxing'an mountains and Zhangguangcai mountains, 28-Qilian orogenic belt.

## Acknowledgments

## Appendix A. Supplementary data

Supplementary data to this article can be found online at https://doi.org/10.1016/j.apgeochem.2018.11.003.

## References

Bi, X.Y., Liu, J.L., Han, Z.X., Yang, W.L., 2015a. Lead in Chinese villager house dust: geographical variation and influencing factors. Environ. Pollut. 207, 183–189.

Bi, X.Y., Li, Z.G., Sun, G.Y., Liu, J.L., Han, Z.X., 2015b. In vitro bioaccessibility of lead in surface dust and implications for human exposure: a comparative study between industrial area and urban district. J. Hazard Mater. 297, 191–197.

Bi, X.Y., Li, Z.G., Wang, S.X., Zhang, L., Xu, R., Liu, J.L., et al., 2017. Pb isotopic compositions of selected coals, Pb/Zn ores and fuels in China and the application for source tracing. Environ. Sci. Technol. 51, 13502–13508.

Caritat, P.de, Cooper, M., Lech, M., McPherson, A., Thun, C., 2009. National Geochemical Survey of Australia: Sample Preparation Manual. Geoscience Australia, pp. 1–27 Record 2009/08.

Caritat, P.de, Cooper, M., 2011. National Geochemical Survey of Australia: the Geochemical Atlas of Australia. Geoscience Australia, Record 2011/20. vol. 1 of 2 Page 56 and 176.

Caritat, P.de, Reimann, C., Smith, D.B., Wang, X.Q., 2018. Chemical elements in the environment: multi-element geochemical datasets from continental- to national-scale surveys on four continents. Appl. Geochem. 89, 150–159.

Chapman, P.M., 2007. Heavy metal - music, not science. Environ. Sci. Technol. 41 (12), 6c.

Chen, H., Teng, Y., Lu, S., Wang, Y., Wang, J., 2015. Contamination features and health risk of soil heavy metals in China. Sci. Total Environ. 512–513, 143–153.

Cheng, H.X., Shen, X.C., Yan, G.S., Gu, T.X., Lai, Z.M., Xie, X.J., 1997. Wide-spaced floodplain sediment sampling covering the whole of China: pilot survey for international geochemical mapping. In: In: Xie, Xuejing (Ed.), Proceedings of the 30th International Geological Congress. Geochemistry, vol. 19. pp. 89–109.

Cheng, H., Li, M., Zhao, C., Li, K., Peng, M., Qin, A., et al., 2014. Overview of trace metals in the urban soil of 31 metropolises in China. J. Geochem. Explor. 139, 31–52.

Chiodo, L.M., Covington, C., Sokol, R.J., Hannigan, J.H., Jannise, J., Ager, J., et al., 2007. Blood lead levels and specific attention effects in young children. Neurotoxicol. Teratol. 29 (5), 538–546.

Chi, Q.H., Yan, M.C., 2007. Handbook of Elemental Abundance for Applied Geochemistry. Geological Publishing House, Beijing (in Chinese).

Clarke, F.W., 1889. The relative abundance of the chemical elements. In: Phil. Soc. Washington Bull. XI, pp. 131–142.

Clarke, F.W., Washington, H.S., 1924. The Composition of the Earth's Crust. USGS Professional Paper 127.

CNEMC (China National Environment Monitoring Center), 1990. Soil Element Background Value in China. China Environment Science Press, Beijing (in Chinese).

Darnley, A.G., Björklund, A., Bølviken, B., Gustavsson, N., Koval, P.V., Plant, J.A., et al., 1995. A Global Geochemical Database for Environmental and Resource Management: Final Report of IGCP Project 259. Earth Sciences, vol. 19 UNESCO Publishing, Paris. http://www.globalgeochemicalbaselines.eu/wp-content/uploads/2012/07/Blue_Book_GGD_IGCP259.pdf.

Duffus, J.H., 2002. 'Heavy Metals' - a meaningless term? Pure Appl. Chem. 74 (5), 793–807.

Fabian, K., Reimann, C., Caritat, P.de, 2017. Quantifying diffuse contamination: method and application to Pb in soil. Environ. Sci. Technol. 51, 6719–6726.

Fortescue, J.A.C., 1992. Landscape geochemistry: retrospect and prospect-1990. Appl. Geochem. 7, 1–53.

Goldschmidt, V.M., 1954. Geochemistry. Clarendon Press, Oxford, pp. 1954.

Goldschmidt, V.M., 1933. Grundlagen der quantitativen Geochemic. Fortschr. Mineral. Kristall. Petrogr. 17, 112–156.

Han, Z.X., Bi, X.Y., Li, Z.G., Yang, W.L., Wang, L.X., Yang, H., et al., 2012. Occurrence, speciation and bioaccessibility of lead in Chinese rural household dust and the associated health risk to children. Atmos. Environ. 46, 65–70.

Han, Z.X., Guo, X.Y., Zhang, B.M., Liao, J.G., Nie, L.S., 2018. Blood lead levels of children in urban and suburban areas in China (1997–2015): temporal and spatial variations and influencing factors. Sci. Total Environ. 625, 1659–1666.

Hu, R., Peng, J., Ma, D., Su, W., Shi, C., Bi, X., 2007. Epoch of large-scale low temperature mineralizations in southwestern Yangtze massif. Miner. Deposits 26 (6), 583–596 (in Chinese with English abstract).

Huang, Z., Hu, R., Su, W., Wen, H., Liu, S., Fu, Y.Z., 2011. A study on the Large-scale Low temperature Metallogenic domain in Southwestern China-Significance, history and new progress. Acta Mineral. Sin. 31 (3), 309–314 (in Chinese with English abstract).

Kasanzu, C., Maboko, M.A.H., Manya, S., 2008. Geochemistry of fine-grained clastic sedimentary rocks of the Neoproterozoic Ikorongo Group, NE Tanzania: implications for provenance and source rock weathering. Precambrian Res. 164, 201–213.

Kushwaha, A., Hans, N., Kumar, S., Rani, R., 2018. A critical review on speciation, mobilization and toxicity of lead in soil microbe-plant system and bioremediation strategies. Ecotoxicol. Environ. Saf. 147, 1035–1045.

Laidlaw, M.A.S., Taylor, M.P., 2011. Potential for childhood lead poisoning in the inner cities of Australia due to exposure to lead in soil dust. Environ. Pollut. 159, 1–9.

Li, Q., Cheng, H.G., Zhou, T., Lin, C.Y., Guo, S., 2012. The estimated atmospheric lead emissions in China, 1990-2009. Atmos. Environ. 60, 1–8.

Li, Z.Y., Ma, Z.W., van der Kuijp, T.J., Yuan, Z.W., Huang, L., 2014. A review of soil heavy metal pollution from mines in China: pollution and health risk assessment. Sci. Total Environ. 468–469, 843–853.

Liu, X., Wang, X., de Caritat, P., Salminen, R., 2015. Comparison of datasets obtained by global-scale geochemical sampling in Australia, China and Europe. J. Geochem. Explor. 148, 1–11.

Mao, J., Bernd, L., Du, A., Zhang, G., Ma, D., Wang, Y., et al., 2002. Re-Os dating of polymetallic Ni-Mo-PGE-Au mineralization in Lower Cambrian black shales of South China and its geologic significance. Econ. Geol. 97, 1051–1061.

Marx, S.K., Rashid, S., Stromsoe, N., 2016. Global-scale patterns in anthropogenic Pb contamination reconstructed from natural archives. Environ. Pollut. 213, 283–298.

Mielke, H.W., Gonzales, C.R., Powell, E., Jartun, M., Mielke Jr., P.W., 2007. Nonlinear association between soil lead and blood lead of children in metropolitan New Orleans, Louisiana: 2000–2005. Sci. Total Environ. 388, 43–53.

Mielke, H.W., Covington, T.P., Mielke Jr., P.W., Wolman, F.J., Powell, E.T., Gonzales, C.R., 2011. Soil intervention as a strategy for lead exposure prevention: the New Orleans lead-safe childcare playground project. Environ. Pollut. 159, 2071–2077.

Needleman, H., 2004. Lead poisoning. Annu. Rev. Med. 55, 209–222.

Négrel, Ph, Sadeghi, M., Ladenberger, A., Reimann, C., Manfred, B., the GEMAS Project Team, 2015. Geochemical fingerprinting and source discrimination of agricultural soils at continental scale. Chem. Geol. 396, 1–15.

Nesbitt, H.W., Young, G.M., 1982. Early Proterozoic climates and plate motion inferred from major element chemistry of lutites. Nature 299, 715–717.

Reimann, C., Matschullat, J., Bike, M., Salminen, R., 2009. Arsenic distribution in the environment: the effects of scale. Appl. Geochem. 24, 1147–1167.

Reimann, C., Flem, B., Fabian, K., Birke, M., Ladenberger, A., Negrel, P., Demetriades, A., Hoogewerff, J., GEMAS Project Team, 2012a. Lead and lead isotopes in agricultural soils of Europe - the continental perspective. Appl. Geochem. 27, 532–542.

Reimann, C., Caritat, P.de, GEMAS Project Team and NGSA Project Team, 2012b. New soil composition data for Europe and Australia: demonstrating comparability, identifying continental-scale processes and learning lessons for global geochemical mapping. Sci. Total Environ. 416, 239–252.

Reimann, C., Birke, M., Demetriades, A., Filzmoser, P., O'connor, P. (Eds.), 2014. Chemistry of Europe's Agricultural Soils. Part A: Methodology and Interpretation of the GEMAS Data Set, vol. 102. Schweizerbart, Stuttgart, pp. 528pp Geologisches Jahrbuch, Reihe B, Heft.

Reimann, C., Birke, M., Demetriades, A., Filzmoser, P., O'connor, P. (Eds.), 2014. Chemistry of Europe's Agricultural Soils. Part B: General Background Information and Further Interpretation of the GEMAS Data Set, vol. 103. Schweizerbart, Stuttgart, pp. 352 Geologisches Jahrbuch, Reihe B, Heft.

Reimann, C., Caritat, P.de, 2017. Establishing geochemical background variation and threshold values for 59 elements in Australian surface soil. Sci. Total Environ. 578, 633–648.

Ren, H., Wang, J., Zhang, X., 2006. Assessment of soil lead exposure in children in Shenyang, China. Environ. Pollut. 144, 327–335.

Rudnick, R.L., Gao, S., 2003. The composition of the continental crust. In: In: Holland, H.D., Condie, K. (Eds.), The Crust, vol. 3. Treatise on Geochemistry. Elsevier Pergamon, Amsterdam, pp. 1–64.

Salminen, R., 2005. Continental-wide geochemical mapping in Europe. Explore 127, 8–15.

Servaraj, K., Arthur, C.C., 2006. Moderate chemical weathering of subtropical Taiwan: constraints from solid-phase geochemistry of sediments and sedimentary rocks. J. Geol. 114, 101–116.

Shaw, D.M., Cramer, J.J., Higgins, M.D., Truscott, M.G., 1986. Composition of the Canadian precambrian shield and the continental crust of the earth. In: In: Dawson, J.B., Carswell, D.A., Hall, J., Wedepohl, K.H. (Eds.), The Nature of the Lower Continental Crust, vol. 24. Geological Society Special Publication, London, pp.

275–282.

Shi, C.Y., Yan, M.C., Liu, C., Chi, Q.H., Hu, S.Q., Gu, T.X., et al., 2005. Abundances of chemical elements in granitoids of China and their characteristics. Geochimica 34 (5), 470–482 (in Chinese with English abstract).

Smith, D.B., Wang, X.Q., Reeder, S., Demetriades, A., 2012. The IUGS/IAGC task group on global geochemical baselines. Earth Sci. Front. 19 (30), 1–6.

Smith, D.B., Cannon, W.F., Woodruff, L.G., Solano, F., Kilburn, J.E., Fey, D.L., 2013. Geochemical and mineralogical data for soils of the conterminous United States: U.S. 801. Geological Survey Data Series, pp. 19. https://pubs.usgs.gov/ds/801/.

Taylor, S.R., 1964. The abundance of chemical elements in the continental crust: a new table. Geochem. Cosmochim. Acta 28, 1273–1285.

Taylor, S.R., McLenan, S.M., 1985. The Continental Crust: Its Composition and Evolution. Blackwell Scientific Publications, London, pp. 312.

Vinogradov, A.P., 1962. Average concentration of chemical elements in the chief types of igneous rocks of the crust of the Earth. Geochemistry 7 555~571. (in Russian).

Wang, X.Q., Shen, W.J., Zhang, B.M., Nie, L.S., Chi, Q.H., Xu, S.F., 2007. Relationship of geochemical blocks and ore districts: examples from the eastern tianshan metallogenic belt, Xinjiang, China. Earth Sci. Front. 14 (5), 116–120.

Wang, X.Q., 2012. Global geochemical baselines: understanding the past and predicting the future. Earth Sci. Front. 19 (3), 7–18 (in Chinese with English abstract).

Wang, W., Wang, X.Q., Nie, L.S., 2015. Study on methods of making geochemical baseline maps. J. Jilin Univ. (Earth Sci. Ed.) S1, 1511–1513 (in Chinese).

Wang, X.Q., the CGB Sampling Team, 2015. China geochemical baselines: sampling methodology. J. Geochem. Explor. 148, 25–39.

Wang, X.Q., Liu, X.M., Han, Z.X., Zhou, J., Xu, S.F., Zhang, Q., et al., 2015b. Concentration and distribution of mercury in drainage catchment sediment and alluvial soil of China. J. Geochem. Explor. 154, 32–48.

Wang, X.Q., Zhou, J., Xu, S.F., Chi, Q.H., Nie, L.S., Zhang, B.M., et al., 2016. China soil geochemical baselines networks: data characteristics. Chin. Geol. 43 (5), 1469–1480 (in Chinese with English abstract).

Wei, F., Chen, J., Wu, Y., Zheng, C., 1991. Study of soil background value in China. Environ. Sci. 12 (4), 12–19 (in Chinese).

Wedepohl, K.H., 1995. The composition of the continental crust. Geochem. Cosmochim. Acta 59, 1217–1232.

WHO (World Health Organization), 2016. Lead Poisoning and Health. September 2016. Retrieved. , Accessed date: 14 October 2016.

Xie, X.J., Cheng, H.X., 1997. The suitability of floodplain sediment as global sampling medium: evidence from China. In: In: Taylor, Graham F., Davy, Richard (Eds.), Geochemical Exploration 1995. J. Geochem. Explor., vol. 58. pp. 51–62.

Xie, X.J., Cheng, H.X., 2001. Global geochemical mapping and its implementation in the Asia-Pacific region. Appl. Geochem. 16 (11–12), 1309–1321.

Yao, W.S., Xie, X.J., Zhao, P.Z., Bai, J.F., 2014. Global scale geochemical mapping program-Contributions from China. J. Geochem. Explor. 139, 9–20.

Yan, M.C., Chi, Q.H., 2005. The Chemical Composition of the Continental Crust and Rocks in the Eastern Part of China. Science Press, Beijing.

Yin, X.C., 1999. Geographic differential characteristics of background of lead in soil in China. J. Qingdao Univ. (Nat. Sci. Ed.) 12 (2), 82–85 (in Chinese with abstract in English).

Zhang, C., Rui, Z., Chen, Y., Wang, D., Chen, Z., Lou, D., 2013. The main successive strategic bases of resources for Pb-Zn deposits in China. Chin. Geol. 40 (1), 248–271 (in Chinese with English abstract).

Zhang, Q., Bai, J.F., Wang, Y., 2012. Analytical scheme and quality monitoring system for China Geochemical Baselines. Earth Sci. Front. 19 (3), 33–42 (in Chinese with abstract in English).

Zhou, Y., Wang, J., Zeng, H., Zhu, Y., 2015. Spatial characteristics of soil heavy metal pollution in Inner Mongolia, China. Ecol. Environ. Sci. 24 (8), 1381–1387 (in Chinese with English abstract).

Zhu, Z.M., Sun, G.Y., Bi, X.Y., Li, Z.G., Yu, G.H., 2013a. Identification of trace metal pollution in urban dust from kindergartens using magnetic, geochemical and lead isotope analyses. Atmos. Environ. 77, 9–15.

Zhu, Z.M., Li, Z.G., Bi, X.Y., Han, Z.X., Yu, G.H., 2013b. Response of magnetic properties to heavy metal pollution in dust from three industrial cities in China. J. Hazard Mater. 189–198, 246–247.